Cross-helix corrugation: The optimal geometry for effective food thermal processing

# Cross-helix corrugation: The optimal geometry for effective food thermal processing

F. Bozzoli[1,2*], L. Cattani[3], S. Rainieri[1,2]

[1] Department of Engineering and Architecture, University of Parma, Parco Area delle Scienze 181/A I-43124 Parma, Italy
[2] SITEIA.PARMA Interdepartmental Centre, University of Parma, Parco Area delle Scienze 181/A, I-43124 Parma, Italy
[3] CIDEA.PARMA Interdepartmental Centre, University of Parma, Parco Area delle Scienze 181/A, I-43124 Parma, Italy

* E-mail address of the corresponding author: fabio.bozzoli@unipr.it

## Abstract

In the present paper, an innovative and effective heat transfer enhancement technique for food processing, cross-helix profile wall corrugation, is proposed and tested. In the food industry, the two most promising corrugation profiles are the transversal and single-helix ones because they both satisfy hygienic design principles. Among the available wall corrugation techniques, transversal corrugation allows for the highest heat transfer performance, and the spirally corrugated tubes guarantee the easiest manufacturing. For this reason, single-helix corrugated tubes are the most commonly employed in heat exchangers for food processing. The cross-helix profile presented in this work represents an intermediate solution between transversal and single-helix corrugation aimed at combining their positive aspects.

One of the main goals of the current research is to identify an optimal geometry that maximises the heat transfer performance by limiting the pressure drop augmentation for this specific engendering application (i.e., food thermal processing). For this purpose, the effect of the geometrical parameters of the corrugation profile is investigated by varying two of the most influent quantities in terms of heat transfer performance and pressure drop: corrugation depth and corrugation pitch. Six pipes characterised by different cross-helix corrugations are tested. Their performance is evaluated by studying the forced convective heat transfer in the Reynolds and Prandtl numbers ranges (50-14000 and 5–150, respectively), using ethylene glycol, water and a mixture of the two as the working fluids.

The outcomes show that corrugation depth plays a crucial role in enhancing the heat transfer performance of the tested pipes. An optimal geometry is established, and correlations to describe its thermal and fluid flow behaviours are proposed. This optimal geometry shows superior performance to that of the most widely adopted types of corrugation. For the low/intermediate Reynolds number range (i.e., 200–2000), the efficiency of the proposed cross-helix profile is up to three times greater than that of the single helix and is also greater than that of transversally corrugated tubes. These outcomes make cross-helix a recommended option to be used in the design of optimised heat exchangers.

Because the studied geometry is expressly developed for food industry application, a set of measurements is also performed in which apricot juice is adopted as the working fluid. The findings confirm the efficiency of the proposed correlations with non-Newtonian fluid foods and enable them to be extended to a wide range of real food industrial applications.

**Keywords:** Convective heat transfer enhancement, cross-helix corrugated tubes, corrugation, food thermal processing, fouling

## Nomenclature

| | | |
|---|---|---|
| $c_p$ | Fluid-specific heat at constant pressure | $J \cdot kg^{-1} K^{-1}$ |
| $D_{env}$ | Tube envelope diameter | m |
| $e$ | Corrugation depth | m |
| $f$ | Darcy friction factor | - |
| $h$ | Convective heat transfer coefficient | $W \cdot m^{-2} K^{-1}$ |

| | | |
|---|---|---|
| $l$ | Corrugation pitch | m |
| $L$ | Length of pipe | m |
| $m$ | Flow consistency index | $Pa \cdot s^n$ |
| $n$ | Flow behaviour index | - |
| $Nu$ | Asymptotic Nusselt number | - |
| $Nu_x$ | Local Nusselt number along axial coordinate | - |
| $p$ | Pressure | Pa |
| $Pr$ | Prandlt number, $Pr = (c_p \cdot \mu)/\lambda$ | - |
| $q$ | Heat flux exchanged per unit surface | $W \cdot m^{-2}$ |
| $Re$ | Reynolds number | - |
| $Re_g$ | Generalised Reynolds number | - |
| $t$ | Wall thickness | m |
| $x$ | Axial coordinate | m |
| $x^*$ | Dimensionless abscissa | - |
| $w$ | Mean fluid axial velocity | m/s |
| $\varepsilon_f$ | Friction factor enhancement | - |
| $\varepsilon_h$ | Heat transfer enhancement | - |
| $\eta$ | Enhancement efficiency | - |
| $\lambda$ | Thermal conductivity | $W \cdot m^{-1} \cdot K^{-1}$ |
| $\mu$ | Dynamic viscosity | $Pa \cdot s$ |
| $v$ | Kinematic viscosity | $m^{2} \cdot s^{-1}$ |
| $\rho$ | Density | $kg \cdot m^{-3}$ |

*Subscripts*

| | |
|---|---|
| $b$ | Bulk |
| $e$ | Enhanced geometry |
| $i$ | Inlet section |
| $w$ | Wall |
| $x$ | Local value along the curvilinear coordinate $x$ |
| $0$ | Reference geometry |

*Superscripts*

| | |
|---|---|
| $\overline{\square}$ | Averaged |

## 1. Introduction

Convection enhancement is a consolidated engineering research topic, particularly related to single-phase heat transfer modality, that is currently attracting renewed interest in the process manufacturing industry because of the rising cost of energy and raw materials. In fact, in several industrial applications, it is mandatory to adopt appropriate heat transfer augmentation strategies in order to decrease the size and cost of heat exchangers.

A large number of papers related to heat transfer enhancement are available in the open scientific literature, as such as those appearing in textbooks by Webb [1], Bergles [2], Kuppan [3] and Manglik [4]. Innovative techniques for the improvement of forced convection in liquids include the adoption of active devices—driven by mechanical assistance or electrostatic fields (see, for instance, [5])—passive devices—generally based on some appropriate configuration of the interface superficies (see, for instance, [2])—or else a combination of both active and passive methods [1].

Passive techniques are more attractive because no power is required to facilitate the enhancement; among the passive techniques are treated surfaces, wall corrugation, displaced enhancement devices, swirl flow devices, surface tension devices, coiled tubes and flow additives, such as nanofluids [1–4]. Wall corrugation represents the most widely adopted solution in the industrial application of heat exchangers. In fact, wall

corrugation acts as a disturbance source in the flow that significantly enhances the thermal performance of the tube section by limiting the pressure drop augmentation, when compared to other passive techniques, such as those based on insert devices [1]. Its application is particularly interesting for shell and tube heat exchangers due to the ability to very easily implement corrugation on the surface of the pipes that constitute these heat transfer devices. The adoption of tubes with corrugated walls allows for a significant increase of the thermal performance when compared to devices using smooth tubes, which have been thoroughly investigated in the past, proven by the high number of correlations proposed for laminar, transitional and turbulent regimes [6-13].

The main augmentation mechanisms activated by wall corrugation are: the interruption of the thermal boundary layer, the flow mixing due to the onset of secondary swirl flow components, the increase of the heat transfer surface area and, above all, the early onset of a transitional turbulent flow regime [14,15].

In this paper, the authors investigate different types of corrugation profiles in an attempt to identify the optimum geometry that allows for increased thermal performance, limited pressure drop and the cleanability regulatory standards to be met, depending on the different application requirements. Among the different kinds of corrugation used so far are internally grooved tubes [16], axially corrugated tubes [17], converging and diverging tubes [18,19], dimpled tubes [20], spirally corrugated tubes [21-24] and wavy channels [25,26].

In the design of heat exchangers for the food and beverage industry, fouling is a crucial aspect to consider. 'Fouling' is defined as the unwanted build-up of material on a surface. The thermal instability of food ingredients results in the formation of fouling deposits in processing plants. Fouling in the food industry is known to be very severe, and the daily cleaning of equipment is a norm in the majority of food plants to ensure that the product meets stringent quality requirements [27]. During the cleaning of heat exchangers, a water and chemical solution is circulated. The typical approach to cleaning follows these steps: pre-rinse, detergent phase (alkali or acid), intermediate rinse, sanitisation and final water rinse [28]. In order to properly conduct the clean-in-place method in an apparatus (i.e., without disassembly), it is fundamental that the pipes are self-draining and their geometries prevent the stagnation of water and chemical solutions. According to the guidelines produced by the European Hygienic Engineering and Design Group, most heat enhancement techniques are unacceptable for food processing; however, mildly corrugated pipes (i.e., with corrugation radius of more than 3 mm) are compatible due to their ability to be easily drained [29].

In the food industry, the two most promising corrugation profiles are the transversal and single-helix ones because they both satisfy hygienic design principles. Among the available wall corrugation techniques, transversal corrugation allows for the highest heat transfer performance, while spirally corrugated tubes guarantee the easiest manufacturing. Single-helix corrugation is easier to produce than is transversal corrugation because it features a continuous rolling of the tube; producing transversal corrugation, in contrast, requires a discontinuous process. The cross-helix profile presented in the current work represents an intermediate solution between these two corrugation profiles, aiming at combining their positive aspects.

A crucial consideration related to corrugated pipes is that there is a critical flow condition that must be overcome to ensure significant and positive effects; only beyond this condition does the use of the corrugation bring about a substantial benefit in terms of heat transfer. One of the first studies that focused on this point was performed by Goldstein and Sparrow [30] for laminar, transitional and low Reynolds number turbulent flow. They found out that in corrugated wall channels, for a laminar flow regime, the transfer coefficients were only slightly higher than those of a parallel-plate channel configuration. Instead, for turbulent flow, the heat transfer rate was up to three times larger than it was when corrugation was not used. Several other authors subsequently found that corrugated pipes do not present heat transfer enhancement in strictly laminar flow conditions while a significant increase of the heat transfer rate is expected with the transition to an unsteady regime [25,31-33]. They observed that the transition in corrugated pipes is a result of complex interactions between the core fluid and the boundary layer fluid through shear-layer self-sustained oscillations. The critical Reynolds number at which the transition to a time-dependent flow regime happens depends significantly on the geometrical parameters of the pipe.

Guzman and Amon [31] examined the evolution from a laminar to an unstable regime in converging and diverging pipes through numerical simulations, investigating the Reynolds number range 10–850. The authors

concluded that the transition occurred through a chain of partial self-sustained periodic, quasi-periodic and, finally, aperiodic or chaotic regimes. Wang and Vanka [32] numerically studied the heat transfer performance of flow in a periodic array of wavy passages; the authors stated that, by exceeding a critical value of Reynolds number of about 180, a transition occurred. They observed that this passage was characterised by a destabilisation of thermal boundary layers in which the fluid near the wall was substituted with that of the core region, consequently generating a mechanism of heat and mass transfer enhancement. Niceno and Nobile [25] investigated the various types of wavy channels perceived at the onset of the unsteady regime in the Reynolds number range 80–200.

Garcia et al. [33] studied the thermal performance of three kinds of heat transfer augmentation devices based on artificial roughness: corrugated tubes, dimpled tubes and wire coil inserts. The authors observed the appearance of a shift to an unsteady regime in the interval $100 < Re < 200$ for wire coils inserts and $900 < Re < 1000$ for the other two types of roughness. The attainment of the critical value of the Reynolds number and the peculiarities of the transition were decisively influenced by the roughness profile and geometrical characteristics.

Rainieri et al. [21,24] focused their research activities on spiral and transversal corrugations, and they found out that corrugation depth represents the most significant parameter that affects the critical Reynolds number: the Reynolds number decreases as the corrugation depth increases. An exhaustive review of the effect of corrugation on heat transfer and pressure drop, conducted by investigating the influence of geometrical parameters, was also presented by Kareem et al. [34].

As above highlighted, cross-helix corrugation is particularly attractive for food processing because of its ability to enhance heat transfer, its low cost and its ability to be easily manufactured, maintained and cleaned. This kind of corrugation can be easily obtained by rolling the same tube twice, with two helical corrugations evolving in opposite directions. Cross-helix corrugation also satisfies hygienic design principles [29]. However, in the available scientific literature, there is a substantial lack of information about the use of this type of corrugation in food processing applications. Some authors studied the application of this type of corrugation in gas flow [35], but their outcomes cannot be extended to food heat exchangers.

The main objectives of the current research, therefore, are to test the cross-helix profile in wall corrugation with attention to the food industry and to identify the optimal geometry that maximises the heat transfer performance by limiting the pressure drop augmentation.

## 2. Tube geometry and experimental setup

In the current study, six stainless steel type AISI 304 pipes, a length of 3 m and presenting wall corrugation with a cross-helix profile, were tested. This kind of corrugation was obtained by rolling the same tube twice, with two helical corrugations evolving along opposite directions; they were produced using an automatic control that allowed the length and incline of the carving extremity to be varied. Regarding the impact of the corrugation profile, the effects of two of the most influent geometric parameters for this type of wall roughness [2,36-38] were investigated (i.e., pitch, $l$, and corrugation depth, $e$): three different values of corrugation depth, $e$, were considered (i.e., 0.6, 0.8 and 1 mm), with the corrugation pitch, $l$, changing between 13 and 29 mm. These values were chosen according to the typical industrial applications for food processing [38]. In Figure 1, the corrugation profile is schematised; it is considered to be part of the wide class, usually identified as ‘spirally enhanced pipes’.

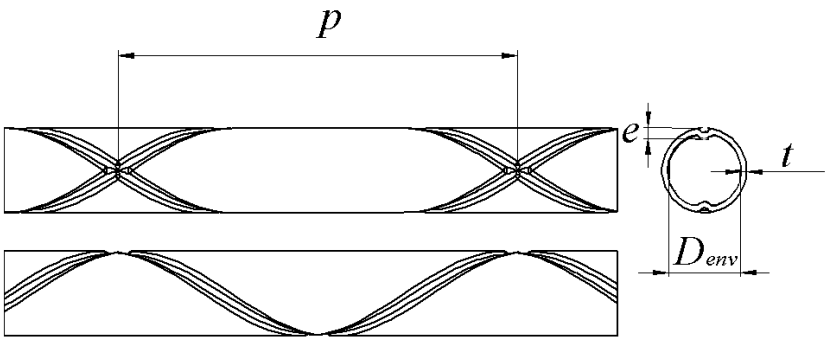


**Figure 1.** Sketch of the wall corrugation profile.

The geometric characteristics of the six studied pipes are summarised in Table 1. They were achieved by carving a smooth tube and are characterised by an internal envelope diameter, $D_{env}$, of 14 mm and a wall thickness, $t$, of 1 mm.

| Tube name | $l$ (mm) | $e$ (mm) | $D_{env}$ (mm) | $t$ (mm) |
|---|---|---|---|---|
| **T1** | 13 | 0.6 | 14 | 1 |
| **T2** | 13 | 0.8 | 14 | 1 |
| **T3** | 13 | 1.0 | 14 | 1 |
| **T4** | 29 | 0.6 | 14 | 1 |
| **T5** | 29 | 0.8 | 14 | 1 |
| **T6** | 29 | 1.0 | 14 | 1 |

**Table 1.** Pipes' geometrical parameters.

Figure 2 illustrates the details of the four representative tubes, highlighting the difference of the corrugation depth and pitch.

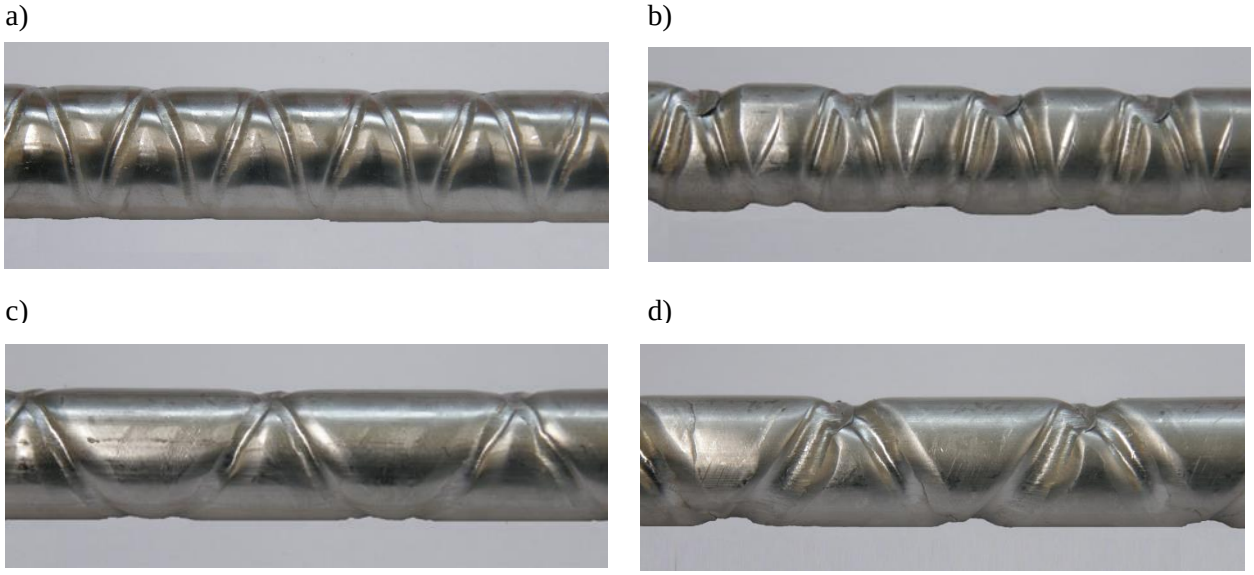


**Figure 2.** Detail of the corrugation profile of tubes T1 (a), T3 (b), T4 (c) and T6 (d).

The performance obtained using the presented corrugation profiles was studied by adopting an experimental setup peculiarly designed for this purpose and schematically reported in Figure 3. The pipes under investigation were kitted out with fin electrodes attached to a power supply (type HP 6671A) that operates in the ranges 0–8 V and 0–220 A. This arrangement was defined to analyse the heat transfer behaviour of the grooved ducts

under the condition of heat generated by the Joule effect in the wall. Attention was paid to the effects related to buoyancy forces, and the selection of the provided heat flux to the working fluid was done to make these forces negligible compared to inertial ones for the fluid velocity values here examined. The temperature of the working fluid was maintained constant at the entrance of the pipe using a secondary heat exchanger supplied with tap water.

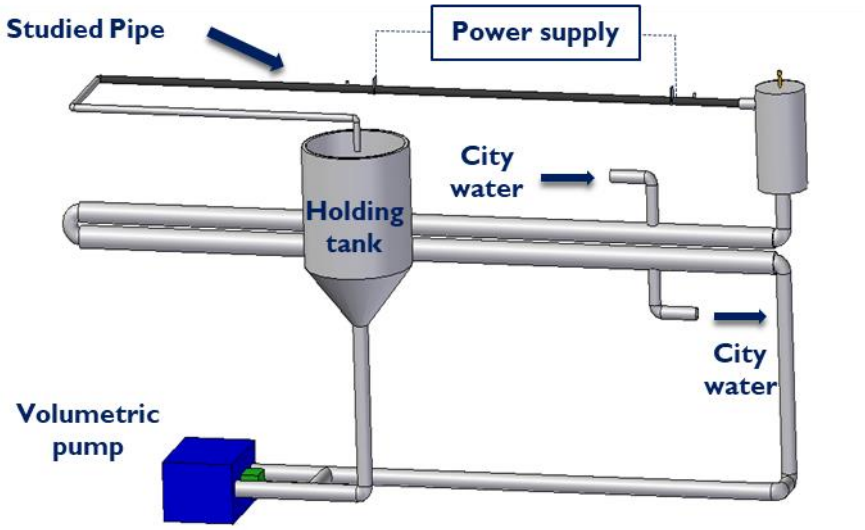


**Figure 3.** Sketch of the experimental setup.

The whole tube was thermally insulated with a double layer of expanded polyurethane with the aim of minimising the heat losses to the environment. Forty T-type thermocouples, calibrated and connected to a multichannel ice point reference (type KAYE K170-50C), were used to measure the temperature of the tube wall and the temperature of the fluid at the inlet and outlet sections.

Concerning the wall temperature, the probes were placed on the external tube's surface at various axial positions along the heated pipe and at different circumferential positions in order to estimate the average temperature of each section. The temperature sensors were positioned externally on the crest of the corrugation along the upper and lower generatrix of the cylindrical envelope's surface. The internal wall temperature was then obtained by solving the steady-state heat conduction problem related to heat generation in the tube wall.

Some thermocouple sensors were positioned on the tube's wall before the heated section to determine the inlet temperature. The bulk temperature at any location in the heat transfer section was calculated from the power supplied to the tube—assumed to be distributed uniformly per unit length over the heat transfer surface area—decreased by the heat losses through the insulation [22]; the outlet temperature was checked also by placing a thermocouple at the end of the heated section. The heat losses towards the environment were estimated in a preliminary calibration of the apparatus with the aim of measuring the overall thermal resistance between the tube wall and the environment. This procedure was performed as follows: in the absence of fluid circulation, a known power rate was supplied to the tube wall, and the difference between the wall temperature and ambient temperature was measured. A value of 6 m K/W was found for the overall thermal resistance that yielded heat losses in the range of 1–3% of the supplied power. In the experimental tests, the wall-to-fluid heat flux varied in the range of $1.0 \cdot 10^3 – 1.1 \cdot 10^4$ W/m$^2$.

Mass flow rate was estimated by timing the interval needed to fill a flask placed at the outlet of the test section, the mass of which was monitored by a high-precision digital balance. Pressure drops in the studied sections were measured using a Rosemount® 3051S differential pressure transducer in isothermal conditions. To investigate the performance of this heat transfer enhancement technique, the forced convective heat transfer

in corrugated wall tubes was studied in the Reynolds and Prandtl numbers ranges of 50–14000 and 5–150, respectively, using ethylene glycol, water and a mixture of the two as working fluids.

In Table 2, the most important properties of the working fluids are summarised for the temperature range of interest in the present study.

| Working fluid | $T$ (°C) | $c_p$ (J·kg$^{-1}$ K$^{-1}$) | $\rho$ (kg·m$^{-3}$) | $\lambda$ (W·m$^{-1}$·K$^{-1}$) | $\mu$ (Pa·s) |
|---|---|---|---|---|---|
| **Water** | 10 | $4.19 \cdot 10^3$ | $1.00 \cdot 10^3$ | 0.59 | $1.3 \cdot 10^{-3}$ |
| | 20 | $4.18 \cdot 10^3$ | $1.00 \cdot 10^3$ | 0.60 | $1.0 \cdot 10^{-3}$ |
| | 30 | $4.18 \cdot 10^3$ | $1.00 \cdot 10^3$ | 0.62 | $0.8 \cdot 10^{-3}$ |
| **Ethylene glycol** | 10 | $1.64 \cdot 10^3$ | $1.18 \cdot 10^3$ | 0.39 | $5.2 \cdot 10^{-2}$ |
| | 20 | $1.67 \cdot 10^3$ | $1.17 \cdot 10^3$ | 0.40 | $2.9 \cdot 10^{-2}$ |
| | 30 | $1.70 \cdot 10^3$ | $1.16 \cdot 10^3$ | 0.41 | $1.8 \cdot 10^{-2}$ |
| **Mixture** | 10 | $2.17 \cdot 10^3$ | $1.11 \cdot 10^3$ | 0.37 | $8.3 \cdot 10^{-3}$ |
| | 20 | $2.18 \cdot 10^3$ | $1.10 \cdot 10^3$ | 0.38 | $6.3 \cdot 10^{-3}$ |
| | 30 | $2.19 \cdot 10^3$ | $1.09 \cdot 10^3$ | 0.39 | $4.2 \cdot 10^{-3}$ |

**Table 2.** Working fluids' properties.

## 3. Data processing

The heat transfer performance and pressure drop drawbacks were assessed in terms of Nusselt number and friction factor, respectively. The envelope diameter, $D_{env}$, that corresponds to the maximum internal diameter was employed as the characteristic length in data processing. To investigate different flow regimes, the experimental tests were conducted by changing the Reynolds number, defined as follows:

$$Re = \frac{\rho \cdot w \cdot D_{env}}{\mu} \tag{1}$$

where $w$ represents the mean fluid axial velocity and $\rho$ and $\mu$ are the density and the dynamic viscosity of the fluid, respectively, evaluated at the average bulk fluid temperature. In relation to the heat transfer behaviour, the local Nusselt number along the axial coordinate was computed as follows:

$$Nu_x = \frac{h_x \cdot D_{env}}{\lambda} \tag{2}$$

where λ is the fluid thermal conductivity evaluated at the local bulk fluid temperature and $h_x$ is the circumferentially averaged local convective heat transfer coefficient, which was determined as follows:

$$h_x = \frac{q}{(\overline{T_w} - T_b)} \tag{3}$$

where $\overline{T_w}$ and $T_b$ are the circumferentially average wall temperature and local bulk fluid temperature, respectively; $\overline{T_w}$ was computed as the mean of the values measured by the two thermocouples placed along the upper and lower generatrix of the cylindrical envelope surface for each axial position. To assess the heat transferred per unit surface area, $q$, the heat exchange area was considered equal to the envelope cylinder's surface area. To estimate the fluid properties, the local fluid bulk temperature was computed as previously described, using the energy balance.

From the distributions of the local Nusselt number, $Nu_x$, it was possible to estimate the average Nusselt number, $\overline{Nu}$, over the heated length and the asymptotic Nusselt number, $Nu$, reached in the fully developed region. In fact, for the experimental arrangements investigated in the present work, the fully developed conditions were always attained in the downstream region of the heated section. In relation to the experimental tests that display spatial fluctuations in the local Nusselt number distribution, an average value in the fully developed region was computed.

The Darcy friction factor, computed as shown in Eq. (4), was adopted as the parameter for evaluating the pressure drops of the studied geometries:

$$f = \frac{\Delta p}{\rho} \cdot \frac{D_{env}}{L} \cdot \frac{2}{w^2} \tag{4}$$

where $\Delta p$ is the pressure drop over the test section having length $L$.

In order to evaluate the improvements and the conceivable drawbacks induced by cross-helix corrugation, it is helpful to refer to two dimensionless quantities usually adopted in the determination of the performance of enhanced geometries [39]: the friction factor and heat transfer enhancement, which are defined as follows:

$$\varepsilon_f = \frac{f_e}{f_0} \tag{5}$$

$$\varepsilon_h = \frac{Nu_e}{Nu_0} \tag{6}$$

where the subscripts *e* and *0* refer to the enhanced and reference geometry, respectively. As reference geometry, a smooth straight tube was used, as is usually assumed in literature [39]; in particular, it was considered that an analytical solution was available for the thermally and hydrodynamically fully developed laminar flow problem [40] in straight smooth wall tubes under a uniform wall heat flux boundary condition and that the Dittus-Boelter correlation was valid for smooth wall tubes in turbulent regimes.

Moreover, an enhancement efficiency following one of the most adopted criteria in the literature [39, 41] was evaluated:

$$\eta = \varepsilon_h / {\varepsilon_f}^{1/3} \tag{7}$$

The uncertainties associated with the directly measured quantities are reported in Table 3.

| $T$ [K] | $\Delta T$ [K] | $\rho$ [kg/m$^3$] | $\mu$ [Pa·s] | $D_{env}$ [m] | $q_g$ [W/m$^3$] | $\dot{V}$ [m$^3$/s] | $\Delta p$ [Pa] |
|---|---|---|---|---|---|---|---|
| ±0.1 | ±0.2 | ±1% | ±1% | ±2% | ±3% | ±1% | 3% |

**Table 3.** The uncertainty of the main physical quantities involved in the estimation procedure.

Applying the propagation of error procedure [42], it was possible to determine the uncertainty of the principal dimensionless group used in this study. The maximum uncertainty for the friction factor, the Nusselt number and the Reynolds number was estimated to be, respectively, ±6%, ±7% and ±3%.

## 4. Results and discussion

### *4.1 Heat Transfer*

In Figure 4, the local Nusselt number, $Nu_x$, distributions (Eq. [2]) are reported along the dimensionless abscissa, defined in Eq. (8). These are conveyed for all the studied pipes for three representative Reynolds number values together with the reference analytical solution of the smooth wall pipe for the thermally and hydrodynamically fully developed laminar flow problem [40].

$$x^* = \frac{x}{Re \cdot Pr \cdot D_{env}} \tag{8}$$

Reynolds number values close to 100 (see Fig. 4a) occurred before the onset of the transitional regime, when the heat transfer performances of all the examined pipes were similar and comparable to smooth wall pipe. As the Reynolds number increased, as shown in Figure 4b ($Re \approx 800–900$), the transition occurred for the tubes with corrugation depths of $e = 0.8$ (T2, T5) and $e = 1$ mm (T3, T6); at this point, the thermal entry region was very limited, and a fully developed flow was promptly reached. The transition to a turbulent regime produced a relevant improvement over the smooth wall performance. Figure 4b also shows that, for the two tubes with the lowest corrugation depth (T1, T4; $e = 0.6$ mm), the heat transfer enhancement was marginal, which could be ascribed to a mild swirling effect produced by the corrugated profile and not to the transition phenomena. On the contrary, for Reynolds number values around 2500–3000, the transition to an unstable regime occurred for all the pipes, as can be seen in Figure 4c.

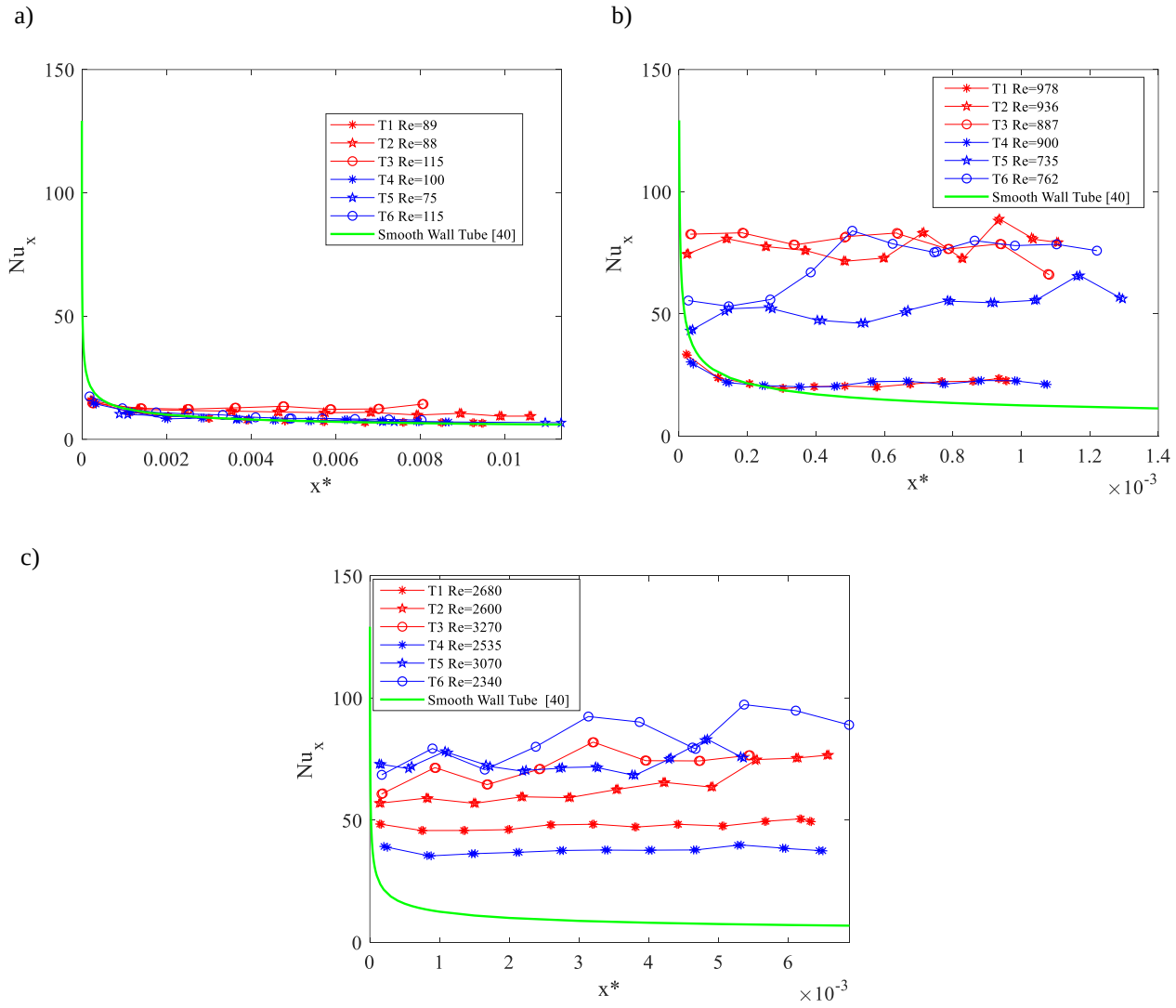


**Figure 4**. The local Nusselt number vs. the dimensionless abscissa $x^*$: a) $Re \approx 100$; b) $Re \approx 800$-$900$; c) $Re \approx 2500$.

To analyse the transitional regime with greater accuracy—and, in particular, to define the critical Reynolds number values that characterise the onset and evolution to an unstable regime for the different pipes—it is more effective to observe the distributions of the asymptotic Nusselt number, shown in figures 5–7. In Figure 5, it is reported that the asymptotic Nusselt number, *Nu*, for all the pipes being studied were in the Reynolds number range of 50–14000. Because the tests were performed using different working fluids (i.e., ethylene glycol, water and mixtures of the two), the asymptotic Nusselt number was divided by $Pr^{1/3}$ to consider the different thermal and physical properties. In the same figure are shown the analytical solutions for the thermally and hydrodynamically fully developed laminar flow problem [40] in smooth wall tubes under a uniform wall heat flux boundary condition and the Dittus–Boelter correlation valid for smooth wall tubes in a turbulent regime [43].

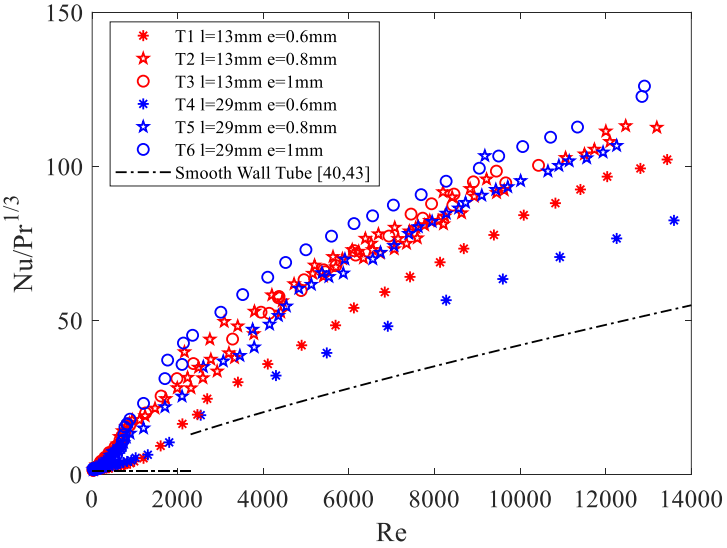


**Figure 5.** Asymptotic Nusselt number divided by $Pr^{1/3}$ in the Reynolds number range 50–14000 and comparison with the smooth wall tubes' behaviour both for laminar [40] and turbulent regimes [43].

For the lower Reynolds number values, the thermal behaviour of all the pipes was comparable; however, when increasing the Reynolds number values, substantial differences arose. The two tubes with the lowest corrugation depth (T1, T4; $e$ = 0.6 mm) were characterised by lower performance when compared with to the tubes with the corrugation depths $e$ = 0.8 (T2, T5) and $e$ = 1 mm (T3, T6).

To better investigate this aspect, it is useful to discuss the results by separately considering two Reynolds number ranges. The first range considered is 50–2300, at which the flow regime for the smooth wall tube is usually considered laminar; the second range is 2300–14000, at which a transition to an unsteady regime and turbulent regime are expected to occur. Figure 6 presents the asymptotic Nusselt number distributions for the Reynolds number range 50–2300. The results are compared with the smooth wall tube behaviour represented by the analytical solution for the thermally and hydrodynamically fully developed laminar flow problem in straight smooth wall tubes under a uniform wall heat flux boundary condition [40].

The data reported in Figure 6 highlight the real impact of cross-helix corrugation on heat transfer performance by producing a significant enhancement. Furthermore, it is also possible to mark the crucial role played by corrugation depth in enhancing the heat transfer features for the ducts under study and to see that corrugation pitch does not appear to have a great influence on the thermal performance of the tested ducts.

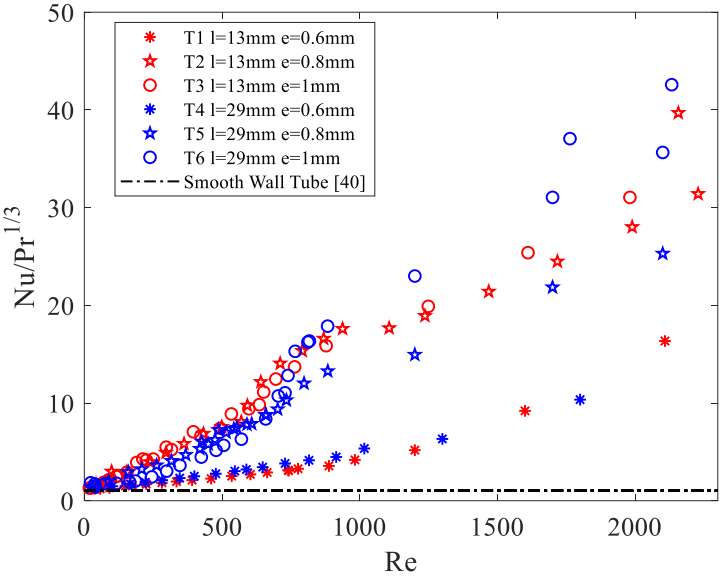


**Figure 6.** Asymptotic Nusselt number divided by $Pr^{1/3}$ in the Reynolds number range of 50–2300.

The results also spotlight that, at a certain corrugation depth (i.e., $e < 0.8$ mm), the wall corrugation outcomes are almost inconsequential for this range of Reynolds number, while at depths greater than this value, the augmentation effect is not intensified.

Furthermore, a very early departure from a laminar to an unstable flow regime was observed for the pipes with corrugation depths of 0.8 and 1 mm; a first departure from the smooth wall behaviour arose around $Re \approx 250$. The transition from a laminar to an unstable flow regime presumably occurred through a series of intermediate steps, as observed in [31]. In fact, a possible second state of transition was present in the range of $600 < Re < 800$. Concerning the effect of the corrugation pitch, it is instead clear that this geometric parameter does not play a significant role in the thermal performance of the tested ducts.

Figure 7 reports the asymptotic Nusselt number distributions for the Reynolds number range 2300–14000. In the same figure, it is also shown that the Dittus–Boelter correlation is valid for smooth wall tubes in a turbulent regime [43]. When increasing the Reynolds number values, the transition to an unsteady regime occurred for the two tubes with the lowest corrugation depth ($e = 0.6$ mm), but their heat transfer performances were still lower than those of the other pipes.

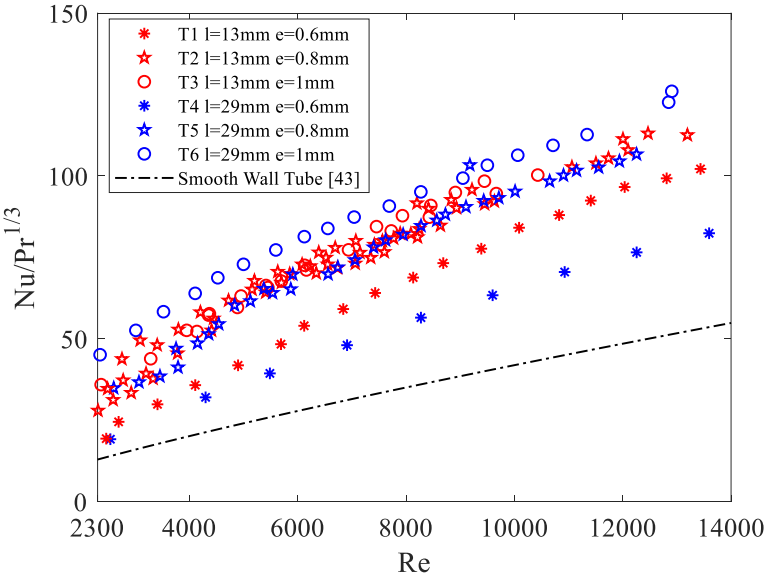


**Figure 7.** Asymptotic Nusselt number divided by $Pr^{1/3}$ in the Reynolds number range of 2300–14000.

Finally, Figure 7 highlights that the ducts with deeper corrugation (i.e., depths equal to 0.8 and 1 mm) also present better thermal performance in the high Reynolds number range.

As observed above, anticipating the transition plays a fundamental role in the heat transfer enhancement mechanism of this kind of passive technique. The main aim of the present paper was to identify an optimum geometry that permits the maximisation of the performance of this type of heat transfer enhancement technique, and it was found that pipes with corrugation depths of $e$ = 0.8 mm and 1 mm are the most favourable.

*4.2 Pressure drop*

Figure 8 shows the average Darcy friction factor for all six of the tested tubes in the Reynolds number range 50–14000, on a bi-logarithmic scale. In the same figure, the analytical solution for the fully developed laminar flow (Eq. [9]) is reported together with the distribution of the friction factor for turbulent regime in a straight tube [43] with the same relative roughness, ε (Eq. [10]). The experimental results obtained with a smooth pipe of the same diameter are also shown.

$$f = 64/Re \tag{9}$$

$$f = \left[-1.8 \cdot log\left(\left(\frac{\varepsilon}{3.7}\right)^{1.11} + \frac{6.9}{Re}\right)\right]^{-2} \tag{10}$$

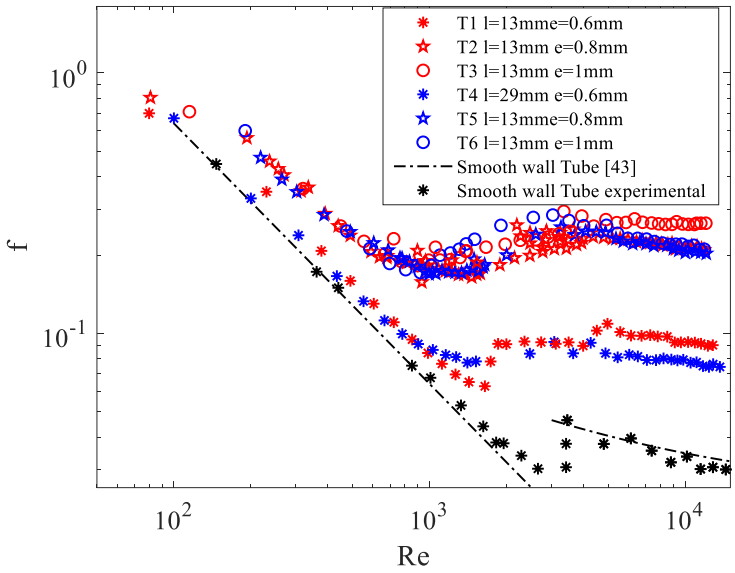


**Figure 8.** Friction factor in the Reynolds number range 50–14000 and comparison with smooth pipe behaviour.

These results conform with the previous observations deduced from the asymptotic Nusselt number distributions: wall corrugation promotes the beginning of an enhanced transitional flow regime in which both heat transfer and pressure drop are increased in comparison with smooth wall behaviour.

To better identify the critical Reynolds number values at which the transition to an intermediate regime occurs, Figure 9 reports the average Darcy friction factor for the two ranges (*Re* 50–2300 and 2300–14000), separately and in a linear scale.

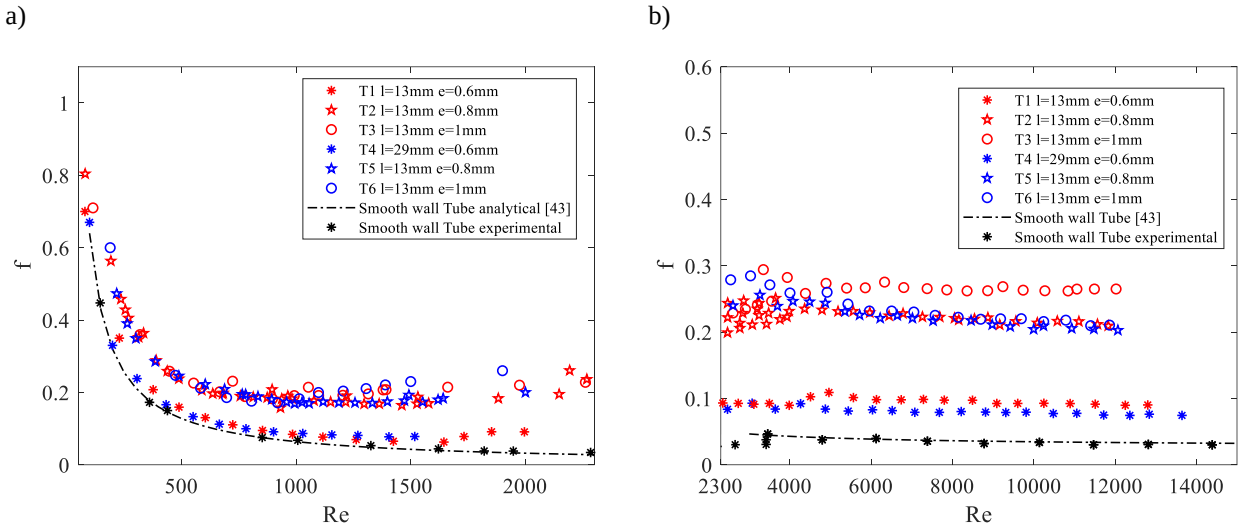


**Figure 9.** Friction factor in the Reynolds number range (a) 50-2300 and (b) 2300-14000.

The tubes with higher values of corrugation depth began to depart from the behaviour of smooth wall tube at Reynolds number values lower than 250, presenting friction factors significantly higher than those of pipes with a corrugation depth of 0.6.

When defining the optimal geometry, attention must also be paid to friction factors because, although the heat transfer performances of tubes T2, T3, T5 and T6 were definitively better than those of tubes T1 and T4, they also present a not negligible drawback in terms of pressure drops.

### *4.3 Enhancement*

To better quantify the improvement of the investigated cross-helix corrugated tubes over a common reference geometry, the friction factor and heat transfer enhancement defined by Eqs. (5,6) were evaluated. The behaviour of $\varepsilon_h$ and $\varepsilon_f$ is reported in Figure 10, in contrast to the Reynolds number, for all the tests conducted.

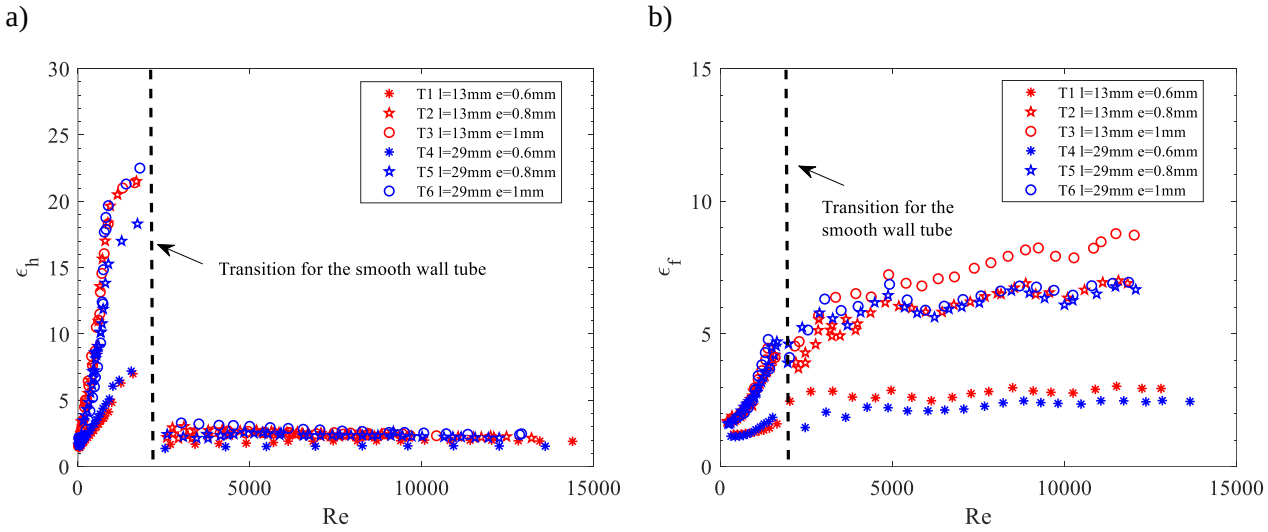


**Figure 10.** Heat transfer enhancement $\varepsilon_h$ (a) and friction factor enhancement $\varepsilon_f$ (b).

The discontinuity in the plot of the $\varepsilon_h$ distribution is due to the fact that, at $Re$ = 2300, the transitional regime for the smooth wall tube begins. For this reason, the reference value $Nu_0$ changes from the asymptotic value for the fully developed laminar flow regime to the value obtained with the Dittus–Boelter correlation that is valid for transitional and turbulent regimes. A discontinuity due to the onset of a transitional regime for the smooth tube at $Re$ = 2300 is also observable for the $\varepsilon_f$ distribution, although less abrupt.

For Reynolds number values lower than 2300, the effect of the depth of wall corrugation on both heat transfer and pressure drops was clearly evident; tubes with a corrugation depth of 0.6 mm presented a heat transfer enhancement in the range of 2-5 against pressure drop augmentation penalties in the range of 1-1.5, while for tubes with higher values of corrugation depth, a heat transfer augmentation of up to 20 was registered against a maximum friction factor increase of 3.5. Similar outcomes for pipes with corrugation depths of 0.8 and 1 mm confirmed the above-described phenomenon. In this Reynolds number range, it is possible to identify the critical value of corrugation depth under which the wall corrugation effects are not significant and beyond which the enhancement does not strongly depend on the severity of the wall corrugation.

At Reynolds number values higher than 2300, where the transition to an unsteady regime is also expected for smooth wall pipes, the values of heat transfer enhancement lessened, and they were all in the range of 1.5–3.5. In contrast, it is still evident that a significant friction factor increase occurred, of between 2 and 3 for a corrugation depth of 0.6 mm and between 5 and 8 for higher values of corrugation depth (see Fig. 10b).

Figure 11 reports the enhancement efficiency, $\eta$, versus the Reynolds number for all six of the tested ducts. These data show that the best tubes were T2, T3, T5, T6 for an $Re < 2300$, while for an $Re > 2300$, tubes T1 and T4 present similar values of $\eta$. Pipes with a corrugation depth of 0.8 mm had almost the same performance as those with a depth of 1 mm, confirming the existence of a critical value of corrugation depth. Considering this, for food applications, mild corrugations are preferred because they provide easier cleanability and maintenance by limiting fouling deposits. As such, the ideal corrugation depth is $e = 0.8$ mm.

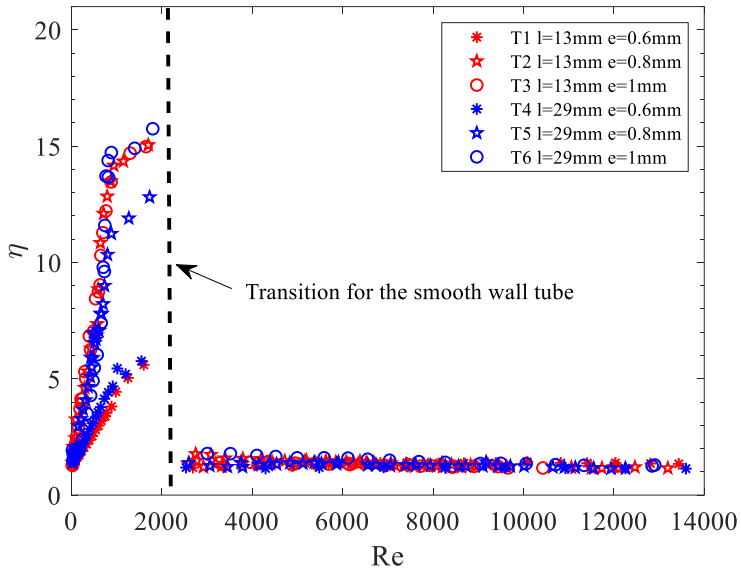


**Figure 11.** Enhancement efficiency, $\eta$.

Regarding the selection of the ideal corrugation pitch, it was observed that it was not possible to spot a clear and univocal effect of the corrugation pitch on either heat transfer or pressure drop; nonetheless, concerning the two pipes with a corrugation depth of 0.8 mm (T2, T5), it was possible to observe a slightly better thermal behaviour in T2 in the laminar regime accompanied by a somewhat more rapid second stage of transition (see Fig. 6). Considering these elements, the optimum selected geometry corresponded to tube T2, for which $e = 0.8$ mm and $l = 13$ mm. The experimental data relating to the selected optimum geometry (T2, $l = 13$ mm, $e = 0.8$ mm) were correlated by considering the dependence of the asymptotic Nusselt number on the Reynolds and Prandtl numbers. The data were managed by employing the multiple linear regression tool within the Matlab environment under the assumption of a power-law dependence of $Nu$ on $Re$ and $Pr$.

For the range $Re < 600$, corresponding to a laminar flow regime, the following correlation was found:

$$Nu = 0.097 \cdot Re^{0.65} \cdot Pr^{0.4} \tag{11}$$

For the range $800 < Re < 14000$, the following correlation, derived by considering the data beyond the transition, was found:

$$Nu = 0.082 \cdot Re^{0.75} \cdot Pr^{0.4} \tag{12}$$

The above correlations are reported together with experimental results in Fig. 12. To estimate the uncertainty of the reported correlation, the 95% confidence interval associated with the Nusselt number assessed via correlations was determined by parametric bootstrap [44], assuming the uncertainties reported at the end of Section 3. The estimated confidence interval for this set of experimental runs was less than ±15%.

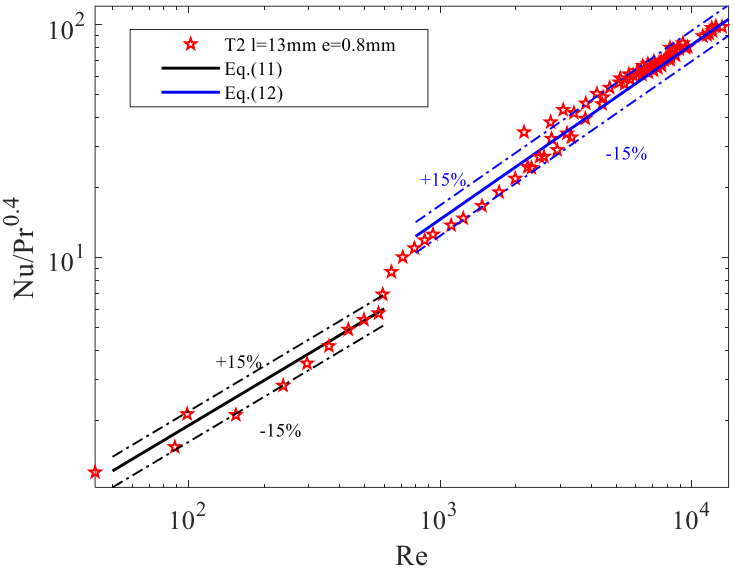


**Figure 12:** Experimental data and optimal correlations for tube T2.

The optimal cross-helix corrugation identified was compared with single-helix corrugation, which is the most common type of corrugation used in food processing, and transversal corrugation, which is considered the most effective type in terms of heat transfer enhancement.

Figure 13 compares, in the range of $50 < Re < 2300$, the three different geometries. In particular, the results obtained by Rainieri et al. [24] and [21] are considered for single-helical corrugation and transversal corrugation behaviour, respectively. Table 4 reports the geometric characteristics of these pipes.

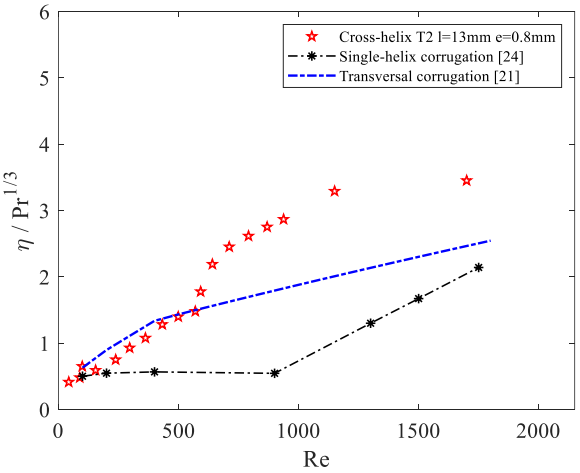


**Figure 13.** Enhancement efficiency for T2 and comparison with the results obtained by Rainieri et al. [24,21].

| Type of roughness single-helix corrugation | $l$ (mm) | $e$ (mm) | $D_{env}$ (mm) |
|---|---|---|---|
| **Optimal double-helix corrugation** | 13 | 0.8 | 14 |
| **Single-helix corrugation [24]** | 13 | 1.0 | 14 |
| **Transversal corrugation [21]** | 16 | 1.5 | 14 |

**Table 4.** Characteristics of the analysed pipes.

The results indicate that, in this Reynolds number range, the heat transfer enhancement obtained for the cross-helix corrugated tubes exceeds the one obtained for the single-helix corrugated tubes, as reported by Rainieri et al. [24]. These data highlight that the cross-helix corrugation profile is more effective than is the single-helix corrugation profile at increasing the heat transfer performance in this Reynolds number range. This augmentation effect it is also promoted by a faster transition to an unstable regime. For the cross-helix profile, as reported in Figure 13, the transitional regime starts around $Re$ = 250 and, through a series of intermediate steps, ends at about $Re$ = 600; in contrast, for the single helix profile, no transition seems to appear before $Re$ = 1200.

The most surprising result is that, in the range of 600 < $Re$ < 2300, the enhancement efficiency of cross-helix corrugation is constantly greater than the value of transversally corrugated pipes. This behaviour could be induced by secondary rotating flows, typical of tubes with spiral corrugation, that are not present when transversal corrugation is present.

As the Reynolds number increased, the differences among cross-helix, single-helix and transversal corrugations decreased in terms of enhanced efficiency. In Figure 14, the enhancement efficiency of optimum cross-helix corrugation is compared with the correlations obtained by Metha et al. [45] for single-helix corrugation and by Chen et al. [17] for transversal corrugation. Table 5 reports the geometric characteristics of these pipes.

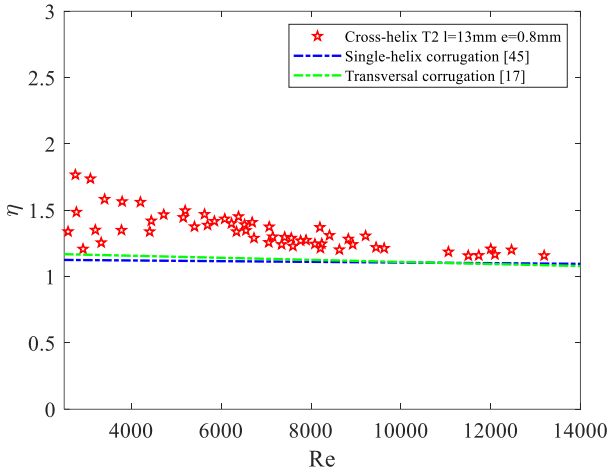


**Figure 14.** Enhancement efficiency for T2 and comparison with the results obtained by Metha et al. [45] and by Chen et al. [17].

| Type of roughness | $l$ (mm) | $e$ (mm) | $D_{env}$ (mm) |
|---|---|---|---|
| **Single-helix corrugation [45]** | 6-12 | 0.16-1.6 | 16 |
| **Transversal [17]** | 16 | 0.75 | 16 |

**Table 5.** Characteristics of the pipes analysed in [45,46].

### *4.4 Experimental test with non-Newtonian food fluid*

Because the studied heat transfer enhancement technique was expressly developed for application in the food industry, a set of measurements was performed adopting real non-Newtonian food fluid as a working fluid in order to verify the correlations previously found. In particular, stabilised apricot juice was used, and its specific density, thermal conductivity, heat and viscosity were measured. Particular attention was paid in the estimation of the viscosity parameters.

As the fluid used is non-Newtonian, the flow consistency index and flow behaviour index needed to be estimated; by means of a rotational rheometer (ARES-TA) these were found to be 0.598 and 0.406, respectively. The generalised Reynolds number values were then calculated as follows:

$$Re_g = 8 \cdot w^{2-n} \cdot \left(\frac{n}{3n+1}\right)^n \cdot \left(\frac{D_{env}}{2}\right)^n \cdot \frac{\rho}{K} \quad (13)$$

where *m* and *n* represent the flow consistency index and the flow behaviour index of the fluid, respectively.

The tests were conducted by adopting the selected optimum geometry, defined above (T2). The results obtained when using apricot juice as the fluid match well with the results obtained when using ethylene glycol, as reported in Figure 15, confirming that the findings of the present study can be reasonably extended to a wide range of real industrial applications.

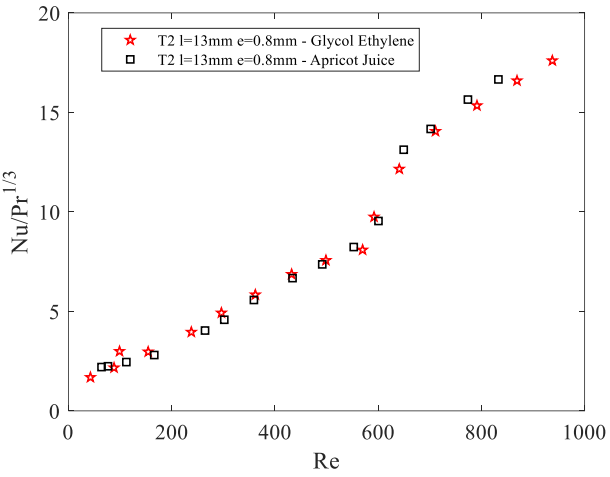


**Figure 15.** Nusselt number obtained using apricot juice.

## 5. Conclusions

Many studies have investigated different corrugation profiles in an attempt to identify the optimum low-cost geometry that increases the thermal performance of heat exchangers while at the same time limiting the pressure drop and continuing to allow cleanability requirements to be met. However, the findings until now have strongly related to specific application requirements. The main objectives of the current research were therefore to test the cross-helix profile in wall corrugation, an effective heat transfer enhancement technique used in food processing.

The influence of the geometrical parameters of the corrugation profile was investigated in terms of heat transfer performance and pressure drops by varying two of the most influent quantities: corrugation depth and corrugation pitch. The outcomes showed that corrugation depth played a crucial role in enhancing the heat transfer performance of the pipes; under a specific corrugation depth (i.e., 0.8 mm), the wall corrugation effects were almost negligible, while beyond that value, the enhancement did not strongly depend on the severity of the wall corrugation. Furthermore, a very early departure from a laminar to an unstable flow regime were observed for the pipes with a corrugation depth above the critical value, with the first departure from the smooth wall behaviour arising around $Re \approx 250$. Moreover, it was observed that the transition from a laminar to an unstable regime occurred through a series of intermediate steps. In fact, a possible second state of transition was present in the range of $600 < Re < 800$. An optimal geometry was identified, and correlations to describe its heat transfer behaviour were proposed.

Because the studied technique was expressly developed for application in heat exchangers in the food industry, a set of measurements were performed adopting apricot juice as the working fluid. The results confirmed that the proposed correlations are valid when real non-Newtonian foods are employed, meaning it is reasonable to extend the proposed correlations to a wide range of industrial applications.

In the food industry, the two most promising corrugation profiles currently used are the transversal and spiral profiles. Between these, transversal corrugation allows for the highest heat transfer performance, while spirally corrugated tubes guarantee the easiest cleaning. From a manufacturing point of view, spiral corrugation is easier to produce than is transversal corrugation because it can be produced by the continuous rolling of the tube; producing transversal corrugation requires a discontinuous process. The optimal cross-helix geometry proposed in the present investigation showed premium performance that topped the performance of the most widely adopted types of corrugation. For a low/intermediate Reynolds numbers range (i.e., 200–2300), the enhancement efficiency of the cross-helix profile is up to three times that of the single-helix profile. Moreover, cross-helix corrugation has an enhancement efficiency that, in the range of $600 < Re < 2300$, is constantly greater than that of transversally corrugated pipes. This behaviour is probably induced by secondary rotating flows, typical of tubes with spiral corrugation. This makes cross-helix corrugation a recommended option to

be used in the design of optimised heat exchangers for food processing because it fulfils all the requirements in terms of high heat transfer potential, low cost, ease of manufacturing and cleanability.

**Acknowledgments**

MBS srl is gratefully acknowledged for the setup of the experimental apparatus. The authors thank Eng. Chiara Freddi for the support given in the experimental work.

**References**

[1] R. Webb, N.H. Kim, Principles of Enhanced Heat Transfer, second Ed., Taylor & Francis, 2005.

[2] A. E. Bergles, Techniques to Enhance Heat Transfer, in: Handbook of Heat Transfer, third Ed., McGraw-Hill, New-York, 1998.

[3] T. Kuppan, Heat Exchanger Design Handbook, Marcel Dekker, Inc. New York, 2000.

[4] R. M. Manglik, Enhancement of Convective Heat Transfer.in: Handbook of Thermal Science and Engineering, 447-477, 2018.

5] S. Rainieri, F. Bozzoli, L. Cattani, P. Vocale, Parameter estimation applied to the heat transfer characterisation of Scraped Surface Heat Exchangers for food applications, Journal of Food Engineering 125 (2014) 147-156.

[6] A. J. Ghajar, K. F. Madon, Pressure drop measurements in the transition region for a circular tube with three different inlet configurations, Experimental thermal and fluid science, 5(1) (1992) 129-135.

[7] A. J. Ghajar, L. M. Tam, Heat transfer measurements and correlations in the transition region for a circular tube with three different inlet configurations, Experimental thermal and fluid science, 8(1) (1994) 79-90.

[8] J. P. Meyer, M. Everts, Single-phase mixed convection of developing and fully developed flow in smooth horizontal circular tubes in the laminar and transitional flow regimes, International Journal of Heat and Mass Transfer, 117 (2018). 1251-1273.

[9] M. Everts, J. P. Meyer, Heat transfer of developing and fully developed flow in smooth horizontal tubes in the transitional flow regime, International Journal of Heat and Mass Transfer, 117 (2018) 1331-1351.

[10] D. Taler, J. Taler, Prediction of heat transfer correlations in a low-loaded plate-fin-and-tube heat exchanger based on flow-thermal tests., Applied Thermal Engineering, 148 (2019) 641-649.

[11] D. Taler, Mathematical modeling and experimental study of heat transfer in a low-duty air-cooled heat exchanger, Energy Conversion and Management, 159 (2018) 232-243.

[12] D. Taler, Numerical modelling and experimental testing of heat exchangers. Springer, 2019.

[13] V. Gnielinski, Heat Transfer in Pipe Flow, VDI Heat Atlas 2nd Ed., pp. 693-699. Chapter G1 Springer-Vieweg Berlin- Heidelberg, 2010.

[14] N. Kurtulmuş, B. Sahin, A review of hydrodynamics and heat transfer through corrugated channels, International Communications in Heat and Mass Transfer, 108 (2019) 104307.

[15] W. T. Ji, A. M. Jacobi, Y. L. He, W. Q. Tao, Summary and evaluation on single-phase heat transfer enhancement techniques of liquid laminar and turbulent pipe flow, International Journal of Heat and Mass Transfer 88 (2015) 735–754.

[16] K. Bilen, M. Cetin, H. Gul, T. Balta, The investigation of groove geometry effect on heat transfer for internally grooved tubes, Applied Thermal Engineering 29 (2009) 753–761.

[17] C. Chen, Y. T. Wu, S.T. Wang, C. F. Ma, Experimental investigation on enhanced heat transfer in transversally corrugated tube with molten salt, Experimental Thermal and Fluid Science, 47 (2013) 108-116.

[18] E. Bellos, C. Tzivanidis, K. A. Antonopoulos, G. Gkinis, Thermal enhancement of solar parabolic trough collectors by using nanofluids and converging-diverging absorber tube, Renewable Energy 94 (2016) 213–222.

[19] G. Pagliarini, P. Vocale, A. Mocerino, S. Rainieri, Second principle approach to the analysis of unsteady flow and heat transfer in a tube with arc-shaped corrugation. In Journal of Physics: Conference Series 796 (2017).

[20] M. Li, T. S. Khan, E. Al-Hajri, Z. H. Ayub, Single phase heat transfer and pressure drop analysis of a dimpled enhanced tube, Applied Thermal Engineering 101 (2016) 38–46.

[21] S. Rainieri, G. Pagliarini, Convective heat transfer to temperature dependent property fluids in the entry region of corrugated tubes, International Journal of Heat and Mass Transfer 45 (2002) 4525–4536

[22] F. Bozzoli, L. Cattani, S. Rainieri, Effect of wall corrugation on local convective heat transfer in coiled tubes. International Journal of Heat and Mass Transfer 101 (2016) 76-90.

[23] S. Rainieri, F. Bozzoli, L. Cattani, G. Pagliarini, Compound convective heat transfer enhancement in helically coiled wall corrugated tubes, International Journal of Heat and Mass Transfer 59 (2013) 353-362.

[24] S. Rainieri, A. Farina, G. Pagliarini, Experimental investigation of heat transfer and pressure drop augmentation for laminar flow in spirally enhanced tubes, Proceedings of the 2nd European Thermal-Sciences and 14th UIT Heat Transfer Conference 1 (1996) 203–209.

[25] N. Niceno, E. Nobile, Numerical analysis of fluid flow and heat transfer in periodic wavy channels, International Journal of Heat and Mass Transfer 22 (2001) 156-167.

[26] Y. Hong, J. Du, S. Wang, S. M. Huang, Heat transfer and flow behaviors of a wavy corrugated tube. Applied Thermal Engineering 126 (2017) 151-166.

[27] P. J. Fryer, K. Asteriadou, A prototype cleaning map: a classification of industrial cleaning rocesses, Trends Food Sci Technol 20 (2009) 225–62.

[28] K. R. Goode, K. Asteriadou, P. T. Robbins, P. J. Fryer, Fouling and cleaning studies in the food and beverage industry classified by cleaning type, Comprehensive Reviews in Food Science and Food Safety 12(2) (2013) 121-143.

[29] European Hygienic Engineering Design Group (EHEDG), 2018. Hygienic design principles. Guideline document No. 8.

[30] L. Goldstein, E. M. Sparrow, Heat/Mass Transfer Characteristics for Flow in a Corrugated Wall Channel, Journal of Heat Transfer 99(2) (1977) 187-195.

[31] A. M. Guzman, C. H. Amon, Dynamic flow characterization of transitional and chaotic regimes in converging-diverging channels, Journal of Fluid Mechanics (1996) 25-57.

[32] G. Wang, S. P. Vanka, Convective heat transfer in periodic wavy passages, International Journal of Heat and Mass Transfer 38 (1995) 3219-3230.

[33] A. Garcia, J. P. Solano, P. G. Vicente, A. Viedma, The influence of artificial roughness shape on heat transfer enhancement: corrugated tubes, dimpled tubes and wire coils, Applied Thermal Engineering 35 (2012) 196-201.

[34] Z. S. Kareem, M. M. Jaafar, T. M. Lazim, S. Abdullah, A. F. Abdulwahid, Passive heat transfer enhancement review in corrugation, Experimental Thermal and Fluid Science, 68 (2015) 22-38.

[35] A. Harleß, E. Franz, M. Breuer, Heat transfer and friction characteristics of fully developed gas flow in cross-corrugated tubes, International Journal of Heat and Mass Transfer 107 (2017) 1076-1084.

[36] N. Tokgoz, M. M. Aksoy, B. Sahin, Investigation of flow characteristics and heat transfer enhancement of corrugated duct geometries, Applied Thermal Engineering 118 (2017) 518-530.

[37] J. G. Withers, E.P. Habdas, Heat transfer characteristics of helical-corrugated tubes for in-tube boiling of refrigerant R-12, AIChE Symposium Series 70 (138) (1974) 98-106.

[38] S. Kakaç, H. Liu, A. Pramuanjaroenkij, Heat exchangers: selection, rating, and thermal design, CRC press 2002.

[39] V. Zimparov, Extended performance evaluation criteria for enhanced heat transfer surfaces: heat transfer through ducts with constant heat flux, International Journal of Heat and Mass Transfer 44(1) (2001) 169-180.

[40] R. K. Shah, A. L. London, Laminar flow forced convection in ducts, Academic Press, 1978.

[41] M. Yilmaz, O.N. Sara, S. Karsli, Performance evaluation criteria for heat exchangers based on second law analysis, Exergy, an International Journal 1(4) (2001) 278-294.

[42] P. R. Bevington, Data Reduction and Error Analysis for the Physical Sciences, McGraw-Hill, 1969.

[43] T. L. Bergman, F. P. Incropera, D. P. DeWitt, A. S. Lavine, Fundamentals of heat and mass transfer. John Wiley & Sons 2011.

[44] B. Efron, The Jackknife, the Bootstrap and Other Resampling Plans, Society of Industrial and Applied Mathematics CBMS-NSFMonographs, Philadelphia, 1982.

[45] M. H. Mehta, M. Raja Rao, Investigations on heat transfer and frictional characteristic of enhanced tubes for condensers, in: Advances in Enhanced Heat Transfer, ASME, New York, 1979.